

Spectra as Windows into Exoplanet Atmospheres

Adam Burrows*

*Princeton University, Princeton, NJ 08544 USA

Accepted to Proceedings of the National Academy of Sciences

Understanding a planet's atmosphere is a necessary condition for understanding not only the planet itself, but also its formation, structure, evolution, and habitability. This puts a premium on obtaining spectra, and developing credible interpretative tools with which to retrieve vital planetary information. However, for exoplanets these twin goals are far from being realized. In this paper, I provide a personal perspective on exoplanet theory and remote sensing via photometry and low-resolution spectroscopy. Though not a review in any sense, this paper highlights the limitations in our knowledge of compositions, thermal profiles, and the effects of stellar irradiation, focussing on, but not restricted to, transiting giant planets. I suggest that the true function of the recent past of exoplanet atmospheric research has been not to constrain planet properties for all time, but to train a new generation of scientists that, by rapid trial and error, is fast establishing a solid future foundation for a robust science of exoplanets.

exoplanets | atmospheres | planetary science | spectroscopy | characterization

Introduction

The study of exoplanets has exponentiated since 1995, a trend that in the short term shows no signs of abating. Astronomers have discovered and provisionally studied more than a hundred *times* more planets outside the solar system than in it. Statistical and orbital distributions of planets across their broad mass and radius continuum, including terrestrial planets/Earths, "super-Earths," "Neptunes," and giants, are emerging at a rapid pace.

However, understanding its atmosphere is a necessary condition for understanding not only the planet itself, but also its formation, evolution, and (where relevant) habitability, and this goal is far from being realized. Despite multiple ground- and space-based campaigns to characterize their thermal, compositional, and circulation patterns (mostly for transiting giant planets), the data gleaned to date have (with very few exceptions) been of marginal utility. The reason for this is that most of the data are low-resolution photometry at a few broad bands that retain major systematic uncertainties and large error bars. Moreover, the theory of their atmospheres has yet to converge to a robust and credible interpretive tool. The upshot of imperfect theory in support of imprecise data has been ambiguity and, at times, dubious retrievals. To be fair, i) telescope assets are being employed with great effort at (and, sometimes, beyond) the limits of their designs; and ii) most planet/star contrast ratios are dauntingly small. As a consequence, the number of hard facts obtained over the last ten years concerning exoplanet atmospheres is small and by no means commensurate with the effort expended.

An important aspect of exoplanets that makes their characterization an extraordinary challenge is that planets are not stars. They have character and greater complexity. A star's major properties are determined once its mass and metallicity are known. Most stars have atmospheres of atoms and their ions. However, planets have molecular atmospheres with elemental compositions that bespeak their formation, accretional, and (where apt) geophysical histories. Anisotropic stellar irradiation, clouds, and rotation can break planetary symmetry severely, with the clouds themselves introducing multiple degrees of complexity, still unresolved even for our Earth. Molecules have much more complicated spectra than atoms, with a hundred to a thousand of

times more lines, and irradiated objects experience complicated photochemistry in their upper reaches. It took stellar atmospheres ~ 100 years to evolve as a discipline, and it still is challenged by uncertainties in oscillator strengths and issues with Boltzmann and thermal equilibrium. Furthermore, the spectroscopic databases for molecules [1], particularly at the high temperatures (500-3500 K) experienced by close-in transiting planets, are much more incomplete than those for atoms, and the relevant collisional excitation rates are all but non-existent. Therefore, it can reasonably be suggested that the necessary theory for detailed studies of exoplanets is in its early infancy.

One might have thought that the study of our solar system had prepared us for exoplanetology, and this is in part true. The solar system has been a great, perhaps necessary, teacher. However, most solar-system spectra are angularly-resolved with a long time baseline and high signal-to-noise. Exoplanets will be point sources for the foreseeable future, and signal-to-noise will remain an issue. Perhaps more importantly, much solar-system research is conducted by probes in-situ or in close orbit, with an array of instruments for direct determination of, for example, composition, surface morphologies, B-fields, charged-particle environments, and gravitational moments. Masses and radii can be exquisitely measured. Orbits are known to standard-setting precision. Moreover, when comparing measured with theoretical spectra, the latter are often informed by direct compositional knowledge.

This is not the scientific landscape that we can envision for exoplanets. Exoplanet science is an observational science that must rely on the astronomical tools of remote spectroscopic sensing to infer the physical properties of individual planets. This puts a premium on obtaining spectra, and developing interpretative toolkits in the tradition of classical astronomy, without the luxury of direct, in-situ probes. Hence, though solar-system variety will continue to inform exoplanet thinking and motivate many calculations, the methodology of solar-system research is not the best model for conducting exoplanet research. Rather, we must determine the most robust and informative methods with which to interpret remote spectra and perform credible spectral retrievals of physical properties. Hence, the science of exoplanet characterization is better viewed as a science of spectral diagnostics, and developing this art should be our future focus.

To date, planets that transit their stars due to the chance orientation of their orbit planes have provided some of the best constraints on hot exoplanet atmospheres. The variation of transit depth¹ and, hence apparent planet radius (R_p), with wavelength (λ) is an ersatz

Reserved for Publication Footnotes

¹equal to the planet/star area ratio, $\left(\frac{R_p}{R_*}\right)^2$, where R_p and R_* are the planet and star radii, respectively – for giants, $\sim 1\%$; for Earths $\sim 0.01\%$.

spectrum and can be used to infer the presence of chemical species with the corresponding cross-sections. Water, sodium, and potassium have been unambiguously detected by this means. Approximately 180° out of phase with the primary transit, when the same planet is eclipsed by its star, the difference between the summed light of planet and star and that of the star alone reveals the planet's light. This is the secondary eclipse, and such measurements, when performed as a function of wavelength, render the planet's emission spectrum; measurements taken between primary and secondary eclipse provide phase light curves. The secondary eclipse planet/star flux ratio is

lower than the transit depth by approximately $\sim \left(\frac{R_p}{2a}\right)^{1/2}$, where a is the orbital semi-major axis and R_* is the stellar radius. This can be a factor of one tenth.

The transit and radial-velocity techniques with which most exoplanets have been found select for those in tight orbits. Tight orbits at the distances of stars in the solar neighborhood subtend very small angles (micro-arcseconds to 10^3 's of milli-arcseconds), and such angular proximity to a bright primary star mitigates against direct planet detection, imaging, or characterization. For wider separations of tens of milliarcseconds to arcseconds, the resulting contrast ratios for terrestrial and giant planets in the optical of $10^{-10} - 10^{-6}$, and in the near- to mid-infrared of $\sim 10^{-8} - 10^{-4}$, are quite challenging[2]. However, such direct planet imaging is not only now conceivable, but has been accomplished. Four giant exoplanets around HR 8799 [3, 4] and one around β Pictoris [5], with masses of $\sim 5 - 15$ Jupiter masses (M_J) and angular separations between ~ 0.3 and ~ 1.5 arcseconds, have recently been found. As direct imaging techniques mature, more and smaller directly-imaged planets will be discovered. However, as articulated earlier, it is only with well-calibrated spectral measurements at useful resolutions that we can hope to characterize wide-separation exoplanet atmospheres robustly. Polarization measurements will also have an important diagnostic role, particularly for cloudy atmospheres, which at quadrature should be polarized in the optical to tens of percent.

Currently, due to their larger size, the photometric and spectroscopic techniques mentioned above have been applied mostly to giant exoplanets. Earths are ten times smaller in radius and one hundred times smaller in mass. Hence, while astronomers and theorists hone their skills on the giant exoplanets, fascinating in their own right, these giants are also serving as stepping stones to the smaller planets, in anticipation of future routine campaigns to characterize them as well. Therefore, I concentrate in this article on the giant population, but all of the basic methodologies employed in their study can be translated bodily to the investigation of smaller "exo-Neptunes," terrestrial planets/Earths, and "super-Earths."

A comprehensive review would necessitate more pages than this more synoptic and summary opinion piece can provide, but for those readers interested in an expanded treatment there are numerous archival papers from which to draw. They cover topics such as the general theory of giant exoplanets [6], giant planet atmospheres [7, 8, 9], analytic atmosphere theory [10, 11], opacities [12, 13, 1], thermochemistry and elemental abundances [14, 15, 16, 17], the chemistry of hot Earth atmospheres [18], albedos [19, 20, 21, 22], giant planet models at wide separations [23, 4, 2], phase functions [24, 25], irradiated atmospheres and inversions [10], basic transit theory [26, 27], transit spectra for Earths [28], emission spectra of Earth-like planets [29], transit spectra of Earth-like planets [30], habitable zones [31], theoretical exo-Neptune spectra [32], planet polarization [33, 20], and clouds and hazes [34, 35, 36]. In this paper, I refer preferentially to my own work, but suggest that the general conclusions arrived at here have broad applicability.

Compositions and Opacities

The variety of compositions found in the gaseous atmospheres of solar-system planets suggests that that for exoplanet atmospheres must be at least as broad. Generally lower in temperature than stellar atmospheres, planetary atmospheres are dominated by molecules.

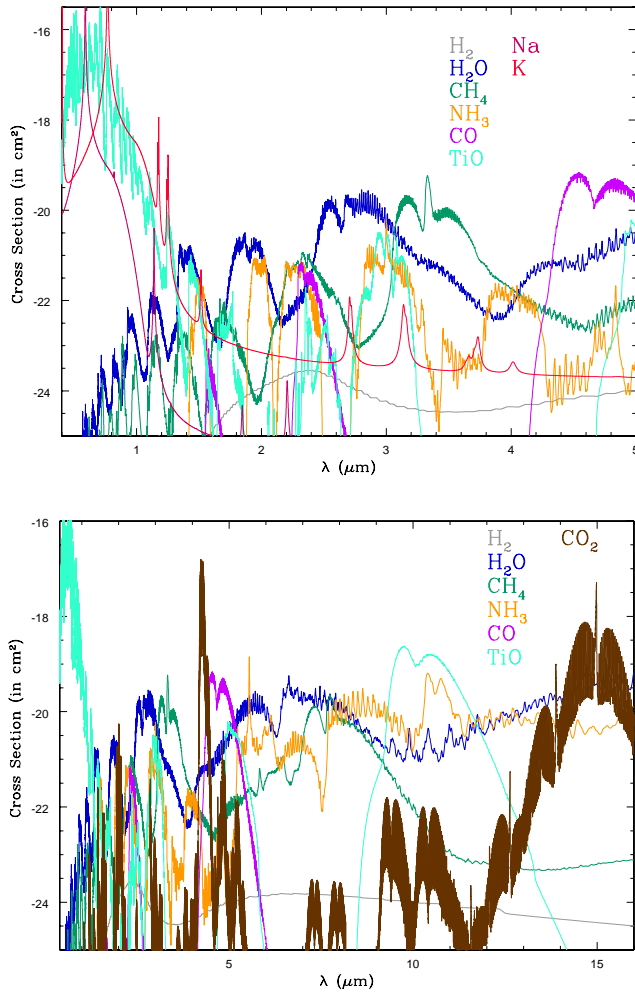


Fig. 1. Top: The figure on the top depicts the logarithm base 10 of the cross section per molecule or atom (in cm^2) versus wavelength (in microns) from 0.4 to $5.0 \mu\text{m}$ for various important species thought to be prominent in the atmospheres of exoplanets, in particular giant exoplanets. They are H_2 (gray), H_2O (blue), CH_4 (green), NH_3 (orange), TiO (cyan), Na (red; leftmost, with strong peak at $0.589 \mu\text{m}$), and K (red; rightmost, with strong peak at $0.77 \mu\text{m}$). Other molecules of note (not depicted) are CO_2 , N_2O , O_2 , and O_3 . For presentation purposes, these cross sections have been calculated at 1500 K and 100 bars. The latter is far too high a pressure to be representative of regions in exoplanet atmospheres that can be probed, but was employed to more clearly distinguish individual features. Importantly, the wavelengths of the major bands and lines are not significantly temperature- or pressure-dependent, though their strengths are. **Bottom:** The figure on the bottom is the same plot, but extended to $16 \mu\text{m}$ to highlight the mid-infrared and to include CO_2 (brown) at 296 K and atmospheric pressure [40]. Note the prominent CO_2 feature at $\sim 15 \mu\text{m}$. The spectral features for each chemical species are crucial discriminating diagnostics for remote exoplanetary sensing and characterization. See text for a discussion.

²It is likely that the brown dwarf and giant planet mass functions overlap, so that a tentative assignment is generally premature. A flexible and open-minded philosophy towards nomenclature is then best[8], which more data will progressively guide towards a more reasonable classification scheme. I do note, however, that much recent data for giant planets has been for the close-in transiting subset. For these, the fact that these are irradiated, while free-floating brown dwarfs are not, significantly alters the colors and atmospheric characteristics of the former, when they might otherwise have had spectra like isolated low-mass brown dwarfs (see figures in the Supplement). One can speculate that, barring the irradiation difference, differences in atmospheric abundances, rotation rates, and orbital regimes might eventually distinguish brown dwarfs from giant planets (at least statistically).

Though fractionation and differentiation processes are no doubt involved in their formation, their elemental abundances should reflect the most abundant elements in the Universe. For giant exoplanets (like brown dwarfs²), this means H₂, He, H₂O, CO, CH₄, NH₃, PH₃, H₂S, Na, K predominate, with most of the metals sequestered in refractories at depths not easily penetrated spectroscopically. However, titanium and vanadium oxides (TiO and VO), identified in cool-star and hot-brown-dwarf atmospheres, have been suggested to reside in quantity in the upper atmospheres of some hot Jupiters to heat them by absorption in the optical and create inversions[37]. However, TiO and VO too are likely condensed out [38]. Since such inversions require an optical absorber at altitude, what this absorber is, molecule or absorbing haze/cloud, remains a major mystery[39].

For terrestrial planets, the molecules N₂, CO₂, O₂, O₃, N₂O, and HNO₃ must be added to the list above, with O₂, O₃ (ozone), and N₂O considered biosignatures, along with the “chlorophyll red edge” (or its generalization). Many other compounds could be envisioned, and there is added complexity to terrestrial planet atmospheres due to atmosphere-surface interactions that are so important, for example, for our Earth. The major constituents of “Neptune” atmospheres are likely closer to those of giants, but the relative abundances in any exoplanet atmosphere must be considered as yet poorly constrained. Constraining these abundances is a goal, however, and one does so by identifying their unique signatures in measured atmospheric spectra and comparing the observed spectrum in its totality with spectral models. This extraction is “retrieval,” which at a minimum should also yield temperatures and temperature profiles. Since many parameters characterize exoplanet atmospheres (e.g., species, abundances, temperatures, spatial distributions, gravities, haze and cloud layers), the low information content of few-band photometry is not adequate to avoid the pitfalls of parameter degeneracy. This, however, with very few exceptions, is the current situation in exoplanet research. With too few data points in pursuit of too many quantities, interpretation is thereby severely compromised and error-prone. It is only with good-resolution spectra, with small and credible error bars, that we can establish robust conclusions about exoplanets and build a solid future for the subject. This is a challenge, but a necessity.

Helium and N₂ have weak spectral features. A prominent O₂ feature is the Fraunhofer A-band at 0.76 μm, and the signal feature for O₃ is the band at 9.6 μm. Rayleigh scattering off molecules roughly follows a λ⁻⁴ dependence, is proportional to the summed product of molecular polarizability and abundance, and is most relevant only in the blue and UV in reflection.

Figure 1 depicts example gas-phase absorption cross sections per molecule (or atom) versus wavelength [13, 1] for H₂, H₂O, CH₄, CO, Na, K, and CO₂ [40]. These species are expected to be important in giant exoplanet atmospheres (for which we currently have the most data), but are also likely important (to varying degrees) in terrestrial, super-Earth, and exo-Neptune atmospheres. In the top plot, we focus on the 1.0 – 5.0 μm range and include the TiO, Na, and K opacities so prominent in the optical, while the bottom plot extends to 15 μm to reveal the behavior in the mid-infrared and the signature feature of CO₂ at ~15 μm.

As indicated in Figure 1, strong water features are ubiquitous and are found at (roughly) 0.94, 1.0, 1.2, 1.4, 1.9, 2.6, and 5 – 7 microns, defining between them the *I*, *Z*, *J*, *H*, *K*, and *M* bands through which much of ground-based near-infrared astronomy is conducted. Methane has important features at 0.89, 1.0, 1.17, 1.4, 1.7, 2.2, 3.3, and 7.8 microns. Carbon monoxide stands out at 2.3 and 4.5 microns, while CO₂ has diagnostic features near 2.1, 4.3, and 15 microns. Ammonia has many features, but the one at 10.5 microns is most noteworthy. Molecular hydrogen (H₂) has no permanent dipole, but one can be induced by collisions (“collision-induced absorption”) at high pressure, and the result is a family of undulations from ~2.2 to ~20 microns that has been seen in Jupiter, Saturn, and brown dwarfs. A central goal of transit, reflection, or emission spectroscopy of ex-

oplanets is to identify these species (and perhaps infer their abundances) by these distinctive features.

Clouds and Hazes

Condensates can form and reside in exoplanet atmospheres as clouds or hazes [21, 35] and can have a disproportionate influence on spectra. This is because, assembled in a grain, such aggregations can respond coherently to light (depending upon the particle size and wave-length). So, very little areal mass density can translate into a large optical depth and a trace species can loom large. In addition, with a spectrum of particle sizes and enhanced line broadening in the grain, their absorption and scattering cross sections can have a continuum character and veil a wide spectral range. The result can be partial (or complete) muting of the gas-phase spectral features, making understanding condensates and incorporating their effects into models as important as it is difficult. To properly handle the effects of clouds we need to know the condensate species, grain size and shape distributions, the complex index of refraction, and the spatial distribution in the atmosphere. Such knowledge is generally in short supply.

The possibility of water clouds in terrestrial atmospheres is uncontroversial, the presence of ammonia clouds in the atmospheres of Jupiter and Saturn has been observed in detail, and the central role of silicate and iron clouds in brown dwarf L dwarfs is reasonably inferred by their very red infrared colors. These situations are in part informed by known thermochemistry. However, water clouds are expected in cold giant exoplanet and brown dwarf atmospheres [24, 41]; Na₂S and KCl clouds are thought to reside in late T dwarf brown dwarfs; an extra absorber in the optical and at altitude has been invoked to explain the inversions and over-hot atmospheres inferred from the spectra at secondary eclipse of some transiting hot Jupiters[39]; a thick haze envelopes the atmosphere of Saturn’s Titan; and there is a trace absorber in the blue that makes Jupiter and Saturn redder than Neptune or Uranus. None of the causative species in these situations is either known, or if known, well-modeled. The case of Jupiter’s color is a cautionary tale. The factor of two suppression in its reflected blue flux could be due to traces at the part in 10¹⁰ level of either polyacetylenes, sulfur or phosphorus compounds, tholins, or something else [19]. Such leverage by a small (and unknown) “actor” in the interpretation of such a large effect should give one pause, and emphasizes the potential complexity of the task of exoplanet characterization. Photolytic chemistry is likely a cause in Titan’s atmosphere, as in many other contexts, but this is small comfort when designing a modeling effort aimed at anticipating all reasonable possibilities.

Scattering in general is important only in reflection and transit spectra, not in emission, and is most prominent for hazes and clouds. In fact, longward of the ultraviolet (UV), clouds are necessary to give a planet any appreciable reflection albedo above ~1% [19]. Also, in reflection, as a general rule, cloud or UV/blue Rayleigh scattering can yield highly polarized fluxes [20]. The polarized fraction is higher when the absorption fraction is higher and the scattering albedo³ is low, but in this case the overall reflected flux is low. This suggests that polarization might in some circumstances be a useful ancillary diagnostic of exoplanet atmospheres. Unlike for gas species, for many realizations of likely hazes or clouds in exoplanet atmospheres, the scattering albedo can be either high or low, depending upon species and wavelength range, and is frequently high. This suggests that reflection spectra can be dominated by the effects of such layers, and, moreover, that transit spectra can be affected by particulate scattering (as opposed to only absorption). Clearly, one must be aware of the possible presence of clouds and hazes when performing exoplanet spectral retrievals.

³the ratio of the scattering cross section to the total cross section

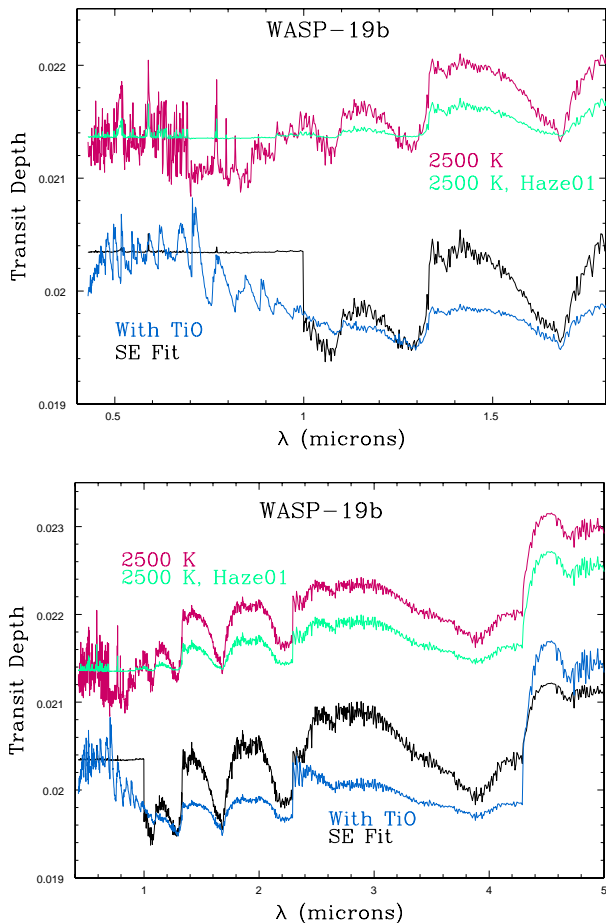


Fig. 2. Top: Shown are model fractional transit depths versus wavelength (in microns) between 0.4 and 1.8 μm for a WASP-19b-like planet. The blue curve is a dayside model with TiO in its atmosphere and a redistribution parameter, P_n , of 0.3[39], that is irradiated by a stellar model of WASP-19 at the distance of WASP-19b. The black curve (“SE Fit”) is a dayside model with a $P_n = 0.3$ and an “extra absorber” at altitude with an opacity of $0.05 \text{ cm}^2 \text{ g}^{-1}$ from 0.4 to 1.0 μm , configured to fit the measured Spitzer/IRAC secondary eclipse data. The red and green models have isothermal atmospheres at 2500 K, with the flatter green model having a uniform haze with an opacity of $0.01 \text{ cm}^2 \text{ g}^{-1}$. **Bottom:** The bottom plot is the same, but extended to 5.0 microns. In all models shown, water features (see Figures 1) are the most prominent, while TiO features are in evidence in the TiO model and the effect of a veiling haze is manifest in that model. Note that for this exoplanet the magnitude of the variation with wavelength is generally less than or equal to a part in a thousand. See text for details.

Transit Spectra

Transit spectra⁴ are direct probes of atmospheric scale heights and atmospheric abundances near the terminator(s). However, if the atmosphere is optically thick and overlays a rocky core there is no obvious way to determine the core’s contribution to the measured radius. Therefore, it is standard practice to analyze transit spectra with respect to an arbitrarily determined reference radius, often taken to be the inferred discovery radius in the optical. When the solid surface of a terrestrial or super-Earth planet is not a priori known, or is inaccessible by measurement, then there will be ambiguity with respect to its contribution to the transit depth. This will not be the case with an airless planet, and is moot for a gaseous planet, but is an issue to consider when falsifying theory.

The measured fractional diminution in the stellar light at a given wavelength is the transit depth [27, 42]. The stellar beams pointed

at the Earth probe the planet’s atmosphere transversely along a chord perpendicular to the impact radius. Hence, the relevant optical depth, τ , is not the depth in the radial direction associated with emission, but much larger. The contribution of the annulus, or partial annulus in the case of the ingress or egress phases, to the blocking of stellar light is $1 - e^{-\tau}$ times the annular area. The sum of such terms over the entire atmosphere provides the integrated blocking fraction due to the atmosphere. That this τ is larger than the radial τ allows transit depth to be more sensitive to trace chemical species than emission or secondary eclipse spectra and amplifies their effect. This may be particularly true of atmospheric hazes that may be too thin in the radial direction to affect emission, but are thick along the chord[43], and may be why Pont et al. [44] see an almost featureless transit spectrum for HD 189733b and infer a veiling haze, while the associated IRAC and IRS data at secondary eclipse clearly reveal water signatures[45]. Another reason may be that since transit spectra probe the terminator, the transition region between day and night, a condensate is more likely to form as the temperature transitions to lower values. Be that as it may, the terminator is a complicated region that introduces special challenges for the theory of transit spectra.

Despite this, a simple analytic model[43, 46, 8] can be developed that captures the basic elements of general transit theory. Integrating along a chord at a given impact parameter and assuming an exponential atmosphere with a pressure scale height, H^5 , yields an approximate amplification factor for the chord optical depth (τ_{chord}) over the radial optical depth of $\sqrt{2\pi R_p/H}$, which can be 5–10. This means that the $\tau_{\text{chord}} = 2/3$ condition that approximately defines the apparent planet radius at a given wavelength is pushed to larger impact parameters (radii) and that the fractional transit depth is increased by a factor $\propto 2H/R_p$. Moreover, it is straightforward to show that

$$\frac{dR_p}{d \ln \lambda} \approx H \frac{d \ln \sigma}{d \ln \lambda}, \quad [1]$$

where σ is the total species-weighted interaction cross section (the sum of absorption and scattering). Note that, whereas emission spectra (ignoring reflection) depend upon only absorption, transit spectra depend upon both scattering and absorption processes. In fact, the haze inferred for HD 189733b could be purely scattering, and as such would make no contribution to the emission at secondary eclipse. However, it is likely that any haze has a non-unity scattering fraction/albedo, introducing flexibility, but also further complexity, into the simultaneous interpretation of transit and emission spectra.

Equation 1 suggests that significant wavelength variations in cross section, as across an absorption band, translate into a change in the apparent radius of order H . This is the essence of the use of transit measurements as a function of wavelength to determine compositions. Since R_p depends upon the logarithm of σ , eq. 1 also indicates that the dependence upon abundance is logarithmic and, hence, weak. While it is “easy” to discern a molecular feature, it is not easy with transit spectra to determine its abundance. Note that since $H = kT/\mu g$, a low (high) temperature, high (low) gravity, or high (low) mean molecular weight atmosphere will yield weaker (stronger) indications of composition. Hence, as long as spectroscopically interesting species reside in the atmosphere in reasonable abundances, a hot, H_2 -rich atmosphere (without a veiling haze/cloud) yields the largest, most diagnostic, radius variations with wavelength.

If there are differences in the compositions and scale heights at the east and west limbs of a planet, such differences are in principle discernible as differences in ingress and egress transit spectra. Though difficult even for a giant exoplanet, such measurements might

⁴Often referred to imprecisely as “transmission spectra.” What one is actually measuring is the transit depth, which reflects what is *not* transmitted. In addition, the implication of the term “transmission” is that we are imaging the planet’s limb region and measuring the variation in τ or $e^{-\tau}$. However, we are actually probing $1 - e^{-\tau}$, its complement.

⁵ $H = kT/\mu g$, where g is the gravity, μ is the mean molecular weight, T is an average atmospheric temperature, and k is Boltzmann’s constant.

be doable in the future and could shed light on atmospheric dynamics and any pronounced zonal flow asymmetries.

In addition, narrow-band, very-high-resolution spectroscopy before and during transit has great potential to reveal planetary orbital, spin, and wind speeds, as well as compositions (cf. the measurement of CO lines by [47]). Though giant exoplanets are the most studied population to date via multi-band transit photometry and spectrophotometry (as opposed to wide single-band observations à la *Kepler* [48]), such data around small M dwarfs for terrestrial planets and super-Earths (such as GJ 1214b – see [43], and references therein) have great promise to probe the atmospheres of these smaller, but likely more numerous, planets. Measuring the emission spectra of Earths around solar-like stars will be much more challenging.

Figures 2 portray the general character of representative theoretical exoplanet transit spectra from 0.4 to 5.0 microns. The models are for the giant WASP-19b and include isothermal atmospheres at $T = 2500$ K, with and without a uniform gray haze with an opacity of $0.01 \text{ cm}^2 \text{ g}^{-1}$, a model that attempts to fit its IRAC data at secondary eclipse [49] with an unknown “extra absorber” at altitude of constant optical opacity $0.05 \text{ cm}^2 \text{ g}^{-1}$ (from 0.4 to 1.0 micron), and a similar model employing TiO as the extra absorber. For clarity, the latter two are shifted arbitrarily from the former two. We note that the transit depth is of order $\sim 2\%$ and that the variation due to the presence of water bands is approximately one part in a thousand. The depths for other hot Jupiters could vary with wavelength by as little as a few parts in ten thousand.

One sees immediately that the extra optical absorber, whatever its nature, increases the ratio of the optical to infrared radii, that the TiO hypothesis can readily be falsified, that the spectral features of (here) water should be readily detected⁶, that the radius variations in the mid-infrared can be of larger amplitude, and that even low-opacity hazes can mute these variations substantially. The diagnostic potential of transit spectra is manifest in plots such as these. It is equally clear that the interpretation of but a few photometric points with significant error bars are ambiguous. Good *spectra* are the key.

Secondary Eclipse

For a circular orbit, when 180° out of phase with the transit, the planet is occulted by the star and is in secondary eclipse. During the eclipse, the summed light of the planet and star being monitored shifts to that of the star alone, and by the difference the planet’s emissions are determined. The *Spitzer* space telescope [51] has been particularly productive in this mode, providing near- and mid-infrared photometric points for ~ 30 nearby transiting planets (mostly giants). For close-in planets, for which the transit probability is largest, the planet is emitting mostly reprocessed stellar light [52, 53]. Stellar irradiation and zonal atmospheric winds and dynamics break the simple spherical symmetry, so that 3D models would seem most appropriate. However, such models have yet to prove themselves and simpler 1D hemisphere-averaged models have been employed, however profitably, to compare with data. Issues with such a prescription include what average flux to employ to derive a representative dayside T/P profile, how to incorporate longitudinal and latitudinal surface flows into the energy budget, non-equilibrium chemistry[56], photochemistry, and day-night differences when interested in total phase curves[53, 54, 55]. Nevertheless, such simple models are still commensurate with the information content of the extant observations.

The various quantities and topics that influence secondary eclipse spectra and have exercised the community include 1) the presence or absence of an extra absorber of currently unknown origin in the upper atmosphere that could heat those regions, at times producing thermal inversions over a restricted pressure range[39, 57]; 2) the temperatures and temperature profiles of the atmosphere; 3) the phase shifts from the orbital ephemeris of the light curves at various wavelengths and spectral bands due to zonal winds that redistribute heat[58]; 4) the compositions and elemental abundances of the atmo-

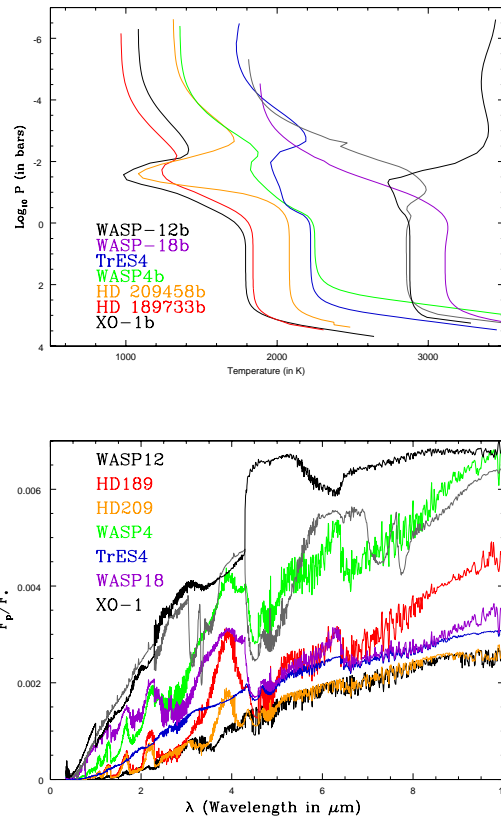


Fig. 3. Top: The top figure portrays model temperature-pressure curves for a collection of transiting giant exoplanets. These models were constructed in an attempt to fit respective *Spitzer*/IRAC data at secondary eclipse and demonstrate the span of temperatures expected in giant exoplanet atmospheres. This span reflects, among other things, the range of sub-stellar fluxes at these given planets, as well as the extra heating of the upper atmosphere by an absorber in the optical that, at times, has been invoked to explain *Spitzer*/IRAC data, in particular at 5.8 microns. Note that the XO-1b model is the black line at the left, while the black line at the right is for WASP-12b with an inversion ($\kappa = 0.1 \text{ cm}^2 \text{ g}^{-1}$), with $P_{\text{in}} = 0.1$, and in chemical and radiative equilibrium at solar elemental abundances. The gray curve is also a model for WASP-12b, but without an inversion, depleted in water by a factor of 100, and enhanced in CH_4 and CO to uniform fractional abundances of 2×10^{-4} . Each model was used to address the WASP-12b IRAC and near-infrared secondary eclipse data. **Bottom:** The planet/star flux ratios from 0.4 to 10 microns for the models on the top. The “predicted” range in values, even for a class of solely giants, is very wide. Note also that comparison between the two WASP-12b models (black and gray) is a cautionary tale against relying too heavily on error-prone photometry to characterize exoplanet atmospheres, and a clarion call for accurate spectra over a wide wavelength range. See text for a discussion.

spheres; 5) the presence of hazes and clouds; 6) the day/night flux contrast; 7) Doppler signatures of atmospheric motions; 8) reflection albedos [59]; and 9) the presence and role of evaporative planetary mass loss. I mention these challenges only to indicate the range of complex problems to be addressed, but will focus in this paper on only the simplest of approaches taken to extract information from secondary-eclipse data.

A few conceptual points are worth noting in passing: 1) An atmosphere calculation with external incident flux will automatically

⁶In fact, water has already been detected in several giant planet atmospheres (e.g., [50]).

⁷ $f = 1/4$ for isotropic models.

generate a reflection albedo and is not extra physics. 2) For a given elemental ratio set, the metallicity dependence of the emergent spectrum is quite weak. Most relevant species (such as water) have one “metal” and incident and emergent integral fluxes must almost balance. 3) The difference between incident and emergent total fluxes is due to the true effective temperature (T_{eff}), which for giant exoplanets of Gigayear ages ranges from 50 to 500 K, and results in a very small contribution to the emergent flux for a strongly irradiated planet. T_{eff} is important only when the stellar irradiation flux is small, and this obtains only for wide-separation planets. 4) The so-called equilibrium temperature, T_{eq} , is defined as the surface black-body temperature for which the incident stellar flux is balanced and is given by

$$T_{\text{eq}} = T_* \left(\frac{R_*}{a} \right)^{1/2} (f(1 - A_B))^{1/4}, \quad [2]$$

where T_* is the stellar effective temperature, f is the heat redistribution factor⁷, and A_B is the Bond albedo[8, 19]. While providing a measure of the mean temperature achieved in a planet’s atmosphere, assuming this can be used as the inner boundary condition T_{eff} has introduced quite a lot of confusion. Very different T/P profiles can yield the same total flux, but very different flux spectra. Figures 4 in the Supplement show two models with the same emergent flux, and, hence, T_{eq} . One consistently incorporates stellar irradiation, while the other puts a flux with $T_{\text{eff}} = T_{\text{eq}}$ at the base of the atmosphere. Both are in radiative and chemical equilibrium. As these figures demonstrate, despite the fact that the emergent fluxes are the same, the corresponding T/P profiles are hugely different and the flux densities at a given wavelength can be off by factors of 2–4! Irradiated atmospheres are different from isolated atmospheres.

Lastly, 5) if an atmosphere is in fact isothermal, there must be an extra absorber in the optical at altitude. Even under irradiation, the temperature gradient must otherwise be negative from base to height, with characteristic temperature changes of ~ 500 – 1500 K for close-in giant exoplanets. Hence, inferences of isothermality are not as content-neutral as is often implied[60].

One can derive an average temperature profile in a radiative-equilibrium exoplanet atmosphere under stellar irradiation by generalizing the classical Milne atmosphere[10, 11]. One obtains:

$$T^4 = \frac{3}{4} T_{\text{eff}}^4 \frac{\kappa_J}{\kappa_B} \left[\tau_R + \frac{1}{\sqrt{3}} \right] + \frac{\kappa_J}{\kappa_B} W T_*^4, \quad [3]$$

where W is the dilution factor, $(R_*/a)^2$, τ_R is the Rossleand depth, κ_J is the photon energy-density weighted opacity, κ_B is the corresponding local black-body-weighted opacity, and we have used the Eddington approximation for the angular moments. For an isolated atmosphere, $\frac{\kappa_J}{\kappa_B}$ is close to one, but for an irradiated atmosphere κ_J and κ_B can differ appreciably. The former at altitude is dominated by the stellar spectrum, while the latter reflects the local atmospheric black-body spectral distribution. If this difference is an interesting function of altitude, an inversion can result[10]. We note that T_{eff} is generally small for close-in hot Jupiters. In this case, the temperatures at depth are determined by the second term, which yields something like eq. (2). In reality, gas giants are convective at high optical depths (~ 100 – 1000) and the T/P profile becomes an adiabat. Otherwise, it would be flat.

Representative theoretical average day-side temperature-pressure profiles for a subset of transiting gas giants are given on the top panel of Figure 3. These are provided to communicate the range of atmospheric temperatures encountered for hot Jupiters and the matching to adiabats at depth above ~ 100 bars. The atmospheres of close-in giants can vary in temperature, depending upon W and T_* , by ~ 1000 – 2000 K. Importantly, the difference in upper atmosphere temperatures between “inverted” and non-inverted situations can be ~ 1000 – 1500 K, a huge difference that can translate into flux spectrum differences of factors of ~ 2 – 4 for ostensibly the same object. This is depicted on the bottom panel of Figure 3, which provides the

corresponding planet/star flux ratios versus wavelength. Among this set of exoplanets, the theoretical flux ratios vary at a given wavelength by an order of magnitude. Moreover, as the comparison between 1) the model for WASP-12b with solar abundances, chemical equilibrium, and an extra upper atmosphere absorber in the optical (upper black) and 2) the model for WASP-12b with enhanced CH_4 and CO , depleted H_2O , and no inversion (gray) attest, mid-infrared planetary spectra can vary significantly for the same stellar irradiation regime and gravity. Figure 3, together with Figure 1, demonstrate the great diagnostic potential of multi-frequency spectra to extract compositions. One can also determine the presence or absence of extra heating by enhanced absorption of stellar light that leads to inversions, but also hotter upper atmospheres and elevated fluxes of features formed in the heated zone. The pronounced bump at ~ 4.5 – 5.5 microns on the inverted spectrum for WASP-12b is due to water in emission and the fact that this band forms where the corresponding temperature profile has a positive (inverted) slope⁸.

Though inversions have been inferred from enhanced *Spitzer* IRAC band fluxes (in particular at 5.8 microns), the nature of the absorber is still unknown. It is suggested that TiO could do it, but there are good reasons to believe this compound would be rained out to depth by various cold traps[38]. There may be a photochemical hazes with the right optical absorbing properties, but this has not been demonstrated. Still, it is tantalizing to hypothesize that the haze inferred by Pont et al.[44] in the atmosphere of HD 189733b and that inferred by Deming et al.[50] in the atmosphere of HD 209458b might in some way be implicated, or at least be of similar composition.

Though the interpretative and diagnostic promise of good spectra is suggested in Figure 3, the current reality is depicted in Figures 5 (in the Supplement). Here, I plot representative measured planet/star flux ratios for 17 transiting giant exoplanets. Most of the data are *Spitzer* IRAC photometry in four bands, while some of the data are from the ground and the Hubble Space Telescope. For HD 189733b, we have *Spitzer*/IRS spectra from ~ 5 to 15 microns as well[45]. To keep the plots from being any more cluttered, error bars for only a few measurements are shown. The quoted $1\text{-}\sigma$ error bars generally range from $\sim 10\%$ to 30% . In an attempt to divide out universal expectations and to focus on what may distinguish one planet from another, I have normalized the planet/star flux ratio with the corresponding black-body value⁹

First, we see from Figures 5 that the normalized ratio is rather flat over a broad range of wavelengths and close to one, perhaps a bit higher. However, the mean level could just reflect the crudeness of the T_p employed for the comparison. We see undulations, but they have little information content, aside from the possible suggestion of enhanced or reduced flux in particular broad spectral regions. The IRS data near 6.2 microns for HD 189733b do imply the presence of water, but what is the feature near 12.5 microns? There is a systematic increase in the ratios to shorter wavelengths, and this is probably real. As supplementary figures 4 imply, fluxes from irradiated planets are expected to be mostly in the near infrared.

The comparison of Figures 3 and 5 starkly emphasizes that we have a long way to go before comparative exoplanetology becomes a richly diagnostic science. At times, data such as are depicted in Figure 5 have been used to find temperatures, compositions, albedos, inversions, carbon-to-oxygen ratios [61], metallicities, and day-night heat redistribution factors, etc. Clearly, these data, and the still primitive state of exoplanet atmosphere theory, do not justify attempts

⁸Emission features won’t always be seen when the extra absorber is active – this depends on where in the atmosphere the band is “formed.”

⁹Dividing by the factor $\frac{j_{\text{bb}}^{\text{bb}}}{j_{\text{bb}}^{\text{bb}}}(\lambda) = \left(\frac{R_p}{R_*} \right)^2 \left(\frac{e^{\frac{hc}{\lambda k T_*}} - 1}{e^{\frac{hc}{\lambda k T_p}} - 1} \right)$, where T_p has been set equal to $T_* \sqrt{\frac{R_*}{2a}}$.

to constrain such quantities simultaneously, or perhaps at all. Until high-quality transit and emission spectra across a wide range of wavelengths are routinely available, only the most primitive and conservative conclusions will be justified. I reiterate that the data in Figures 5 are for giant exoplanets. Smaller Neptunes, super-Earths, and terrestrial planets around similar stars will be much more difficult targets.

Systematic Uncertainties in the Data and Theory

Theorists and observers alike, anxious to extract all the conclusions they can from this first generation of measurements of exoplanet atmospheres, have tended to overinterpret them. A comparison between Figures 3 and 5 is a sober indication of the current limitations of the science. The telescopes being used were not designed with exoplanets in mind. For example, *Spitzer* was designed for photometry at the $\sim 1\%$ level, yet it is being used (however heroically) to obtain numbers at the $\sim 0.1\text{--}0.01\%$ level. Generally, the space-based and ground-based data have limited signal-to-noise, the systematic effects/errors are variously and imperfectly corrected for, there frequently is no absolute calibration across disparate wavelength regions, stellar spots are difficult to account for, and corrections for the Earth's atmosphere for ground-based observations have been problematic. Data for the same object at the same wavelength, but taken by different teams, have varied by up to factors of ~ 2 , and such a factor can completely alter the conclusions drawn about abundances, C/O ratios, inversions, etc.

Given this list of limitations, one should be highly sceptical of extraordinary claims based on imperfect data with low intrinsic information content. Many published model fits have been highly under-constrained. This is all the more important given the gross imperfections in current exoplanet atmosphere theory. With a few photometric points, one can not simultaneously determine with any confidence, or credibly incorporate into the fitting procedures, chemical and elemental abundances, wind dynamics, longitudinal heat redistribution, thermal profiles, albedos, the potential influence of hazes and clouds, non-equilibrium chemistry and photochemistry, and magnetic fields. Furthermore, the opacities for many chemical species are only imperfectly known, convection at depth is frequently handled with a mixing-length approach, and emissions over a planetary hemisphere are never calculated with correct, multi-dimensional radiative transfer. Moreover, most of the current generation of 3D general circulation models (GCMs) filter out sound waves, but derive transonic flows speeds with Mach numbers at and above one without a means to handle shock waves. Many of these codes have also inherited from Earth GCM practice various ad hoc "Rayleigh drag" and hyperdiffusivity terms with arbitrary coefficients calibrated on the Earth that compromise the wind dynamics on strongly irradiated gas giants, even if magnetic torques are sub-dominant. Importantly, GCMs were configured to look at winds and pressures, not spectral emissions, highlighting the mismatch between the traditional goals of planetary and Earth scientists and exoplanet astronomers.

At times, basic atmosphere practice has been shunted aside in attempts to retrieve thermal and compositional information from a few (though precious) data points. Examples are 1) using unphysical, parametrized T/P profiles and arbitrary compositions, while not addressing local energy and chemical balance; 2) using 1D averaged models for what is a 3D planet; 3) using T_{eq} as if it were a real physical quantity of relevance to spectra; 4) defining and deriving a reflection albedo when the planet is mostly emitting thermally; or 5) fitting photometric points with T_{eq} and a Bond albedo. Such approaches might seem right-sized to the data at hand, but are likely to generate an erroneous sense of confidence in the conclusions derived. For example, it is long been known that small errors in ΔT can translate into large spectral flux errors, even if the total reprocessed emitted flux is ostensibly addressed.

The Future

Therefore, I suggest that once high-quality, well-calibrated, stable spectra across a broad range of wavelengths from the optical to the mid-infrared are finally available many conclusions reached recently about exoplanet atmospheres will be overturned. The current interpretations and theories are just not robust enough to survive intact into the future. However, despite the generally cautionary tone of much of this paper, I see an exciting future. The past ~ 20 years has been but a training period for a new generation of exoplanet scientists, forged by trial and error and educated in the new questions posed by exoplanets. Its growing membership is testing its tools — new technologies, concepts, theories, and techniques — that will serve to establish a solid foundation for a true science of planets not tethered to the solar system. Informed by the latter, but optimized to address its unique challenges as a remote-sensing science, comparative planetary's youth is rapidly maturing.

The near- and mid-term future of exoplanet atmosphere characterization will include the James Webb Space Telescope (JWST)[62, 63], ground-based Extremely-Large/Giant-Segmented-Mirror Telescopes (ELTs/GSMTs)[64], and perhaps dedicated Explorer, M-Class (e.g., EchO[65]), or Probe-Class space missions. The continued creative use of existing ground-based telescopes is assured, and new high-contrast coronagraphic imaging programs now coming on line (such as GPI[66] and SPHERE[67]) show great promise. Importantly, there is the exciting possibility of putting a coronagraph on WFIRST/AFTA [68]. In the farther future, once a cost-effective plan can be articulated, a major dedicated space mission of exoplanetary atmosphere characterization, such as was envisioned with the TPFs and Darwin, should be possible. Currently, giant planets and Neptunes pose the most realistic targets, but terrestrial planets and the possibility of discerning signatures of life are majors goal of many. Soon, the spectra of terrestrial planet atmospheres around small M-dwarf stars may be within reach.

Given this, it is clear that, for the field to remain vibrant and grow, it needs a heterogeneous and balanced program of ground-based and space-based facilities and programs. If anything has been demonstrated by the first ~ 20 years of exoplanet research, it is that some of the best techniques for studying them are unanticipated. The transit technique for close-in planets has been a game-changer, but was not envisioned in previous planning documents. High-contrast imaging, only now coming of age, was to inaugurate the era of atmospheric characterization. It is also clear that large, expensive missions are counterproductive until they are demanded by the science, in fact until the science indicates that further progress demands them. Precursor technologies for such missions should certainly be pursued and allowed to compete. But overlarge and expensive missions without the requisite credibility and technological heritage in place can fatally squeeze the smaller programs that have proven so fruitful. This implies that an international Roadmap should be crafted for exoplanet's next ~ 20 years. Its guiding principle should be a balanced approach of small, medium, and large initiatives that encourages flexibility and scientific return, and does not presume (or proscribe) a specific future. The clear goal is to understand in rich detail the planets that we now know exist in profusion in the galaxy and Universe. One is only left to ask: Are we ready to assume the challenge?

ACKNOWLEDGMENTS. The author would like to acknowledge support in part under NASA ATP grant NNX07AG80G, HST grants HST-GO-12181.04-A, HST-GO-12314.03-A, HST-GO-12473.06-A, and HST-GO-12550.02, and JPL/Spitzer Agreements 1417122, 1348668, 1371432, 1377197, and 1439064. A diverse suite of exoplanetary spectral and evolutionary models for a range of masses and compositions is available at <http://www.astro.princeton.edu/~burrows> and from the author upon request.

1. Rothman L S, et al. (2008) The HITRAN 2008 Molecular Spectroscopic Database. *Journal of Quantitative Spectroscopy & Radiative Transfer* 110:533-572.
2. Burrows A (2005) A theoretical look at the direct detection of giant planets outside the Solar System. *Nature* 433:261-268.
3. Marois C et al. (2008) Direct Imaging of Multiple Planets Orbiting the Star HR 8799. *Science* 322:1348-1352.
4. Madhusudhan N, Burrows A, Currie T (2011) Model Atmospheres for Massive Gas Giants with Thick Clouds: Application to the HR 8799 Planets. *Astrophys. J.* 737:34-48.
5. Lagrange A M et al. (2009) A probable giant planet imaged in the β Pictoris disk. VLT/NaCo deep L'-band imaging. *Astron. Astrophys.* 493:L21-L25.
6. Burrows A, et al. (1997) A Non-Gray Theory of Extrasolar Giant Planets and Brown Dwarfs. *Astrophys. J.* 491:856-875.
7. Burrows A, Orton G (2010) *Giant Planet Atmospheres and Spectra* in EXOPLANETS, ed Seager S (Space Science Series of the University of Arizona Press, Tucson), pp. 419-440.
8. Burrows A, Hubbard, W B, Lunine J I (2001) The Theory of Brown Dwarfs and Extrasolar Giant Planets. *Rev. Mod. Phys.* 73:719-765.
9. Sudarsky D, Burrows A, Hubeny I (2003) Theoretical Spectra and Atmospheres of Extrasolar Giant Planets. *Astrophys. J.* 588:1121-1148.
10. Hubeny I, Burrows A, Sudarsky D (2003) A Possible Bifurcation in Atmospheres of Strongly Irradiated Stars and Planets. *Astrophys. J.* 594:1011-1018.
11. Guillot T (2010) On the radiative equilibrium of irradiated planetary atmospheres. *Astron. Astrophys.* 520:A27-A39.
12. Freedman R S, Marley M S, Ladders K (2008) Line and Mean Opacities for Ultracool Dwarfs and Extrasolar Planets. *Astrophys. J. Suppl.* 174:504-513.
13. Sharp C M, Burrows A (2007) Atomic and Molecular Opacities for Brown Dwarf and Giant Planet Atmospheres. *Astrophys. J. Suppl.* 168:140-166.
14. Ladders K (2003) Solar System Abundances and Condensation Temperatures of the Elements. *Astrophys. J.* 591:1220-1247.
15. Ladders K, Fegley B (2002) Atmospheric Chemistry in Giant Planets, Brown Dwarfs, and Low-Mass Dwarf Stars. I. Carbon, Nitrogen, and Oxygen. *Icarus* 155:393-424.
16. Ladders K, Fegley B (1998) *The planetary scientist's companion*. (Oxford University Press, New York).
17. Burrows A, Sharp C (1999) Chemical Equilibrium Abundances in Brown Dwarf and Extrasolar Giant Planet Atmospheres. *Astrophys. J.* 512:843-863.
18. Schaefer L, Fegley B (2009) Chemistry of Silicate Atmospheres of Evaporating Super-Earths. *Astrophys. J. Lett.* 703:L113-L117.
19. Sudarsky D, Burrows A, Pinto P (2000) Albedo and Reflection Spectra of Extrasolar Giant Planets. *Astrophys. J.* 538:885-903.
20. Madhusudhan N, Burrows A (2011) Analytic Models for Albedos, Phase Curves, and Polarization of Reflected Light from Exoplanets. *Astrophys. J.* 747:25-40.
21. Marley M S, Gelino C, Stephens D, Lunine J I, Freedman R (1999) Reflected Spectra and Albedos of Extrasolar Giant Planets. I. Clear and Cloudy Atmospheres. *Astrophys. J.* 513:879-893.
22. Burrows A, Ibgui L, Hubeny I (2008) Optical Albedo Theory of Strongly-Irradiated Giant Planets: The Case of HD 209458b. *Astrophys. J.* 682:1277-1282.
23. Burrows A, Sudarsky D, Hubeny I (2004) Spectra and Diagnostics for the Direct Detection of Wide-Separation Extrasolar Giant Planets. *Astrophys. J.* 609, 407-416.
24. Sudarsky D, Burrows A, Hubeny I, Li A (2005) Phase Functions and Light Curves of Wide Separation Giant Planets. *Astrophys. J.* 627:520-533.
25. Barman T S, Hauschildt P H, Allard F (2005) Phase-Dependent Properties of Extrasolar Planet Atmospheres. *Astrophys. J.* 632:1132-1139.
26. Seager S, Sasselov, D D (2000) Theoretical Transmission Spectra during Extrasolar Giant Planet Transits. *Astrophys. J.* 537:916-921.
27. Brown T (2001) Transmission Spectra as Diagnostics of Extrasolar Giant Planet Atmospheres. *Astrophys. J.* 553:1006-1026.
28. Kaltenegger L, Traub W A (2009) Transits of Earth-like Planets. *Astrophys. J.* 698:519-527.
29. Kaltenegger L, Traub W A, Jucks, K W (2007) Spectral Evolution of an Earth-like Planet. *Astrophys. J.* 658:598-616.
30. Ehrenreich D, Tinetti G, Lecavelier Des Etangs A, Vidal-Madjar A, Selsis F (2006) The transmission spectrum of Earth-size transiting planets. *Astron. Astrophys.* 448:379-393.
31. Kasting J F, Whitmire D P, Reynolds R T (1993) Habitable Zones around Main Sequence Stars. *Icarus* 101:108-128.
32. Spiegel D, Burrows A, Ibgui L, Hubeny I, Milsom J A (2009) Models of Neptune-Mass Exoplanets: Emergent Fluxes and Albedos. *Astrophys. J.* 709:149-158.
33. Seager S, Whitney B A, Sasselov D D (2000) Photometric Light Curves and Polarization of Close-in Extrasolar Giant Planets. *Astrophys. J.* 540:504-520.
34. Ackerman A S, Marley M S (2001) Precipitating Condensation Clouds in Substellar Atmospheres. *Astrophys. J.* 556:872-884.
35. Marley M S, Ackerman A S, Cuzzi J N, Kitzmann D (2013) Clouds and Hazes in Exoplanet Atmospheres. in "Comparative Climatology of Terrestrial Planets," eds. S Mackwell, M Bullock, J Harder (University of Arizona Press, Tucson), pp. XXX-YYY (arXiv1301.5627).
36. Helling C et al. (2008) A comparison of chemistry and dust cloud formation in ultracool dwarf model atmospheres. *Mon. Not. R. Astron. Soc.* 391:1854-1873.
37. Fortney, J J, Ladders K, Marley M S, Freedman R S (2008) A Unified Theory for the Atmospheres of the Hot and Very Hot Jupiters: Two Classes of Irradiated Atmospheres. *Astrophys. J.* 678:1419-1435.
38. Spiegel D, Silverio K, Burrows A (2009) Can TiO Explain Thermal Inversions in the Upper Atmospheres of Irradiated Giant Planets? *Astrophys. J.* 699:1487-1500.
39. Burrows A, Hubeny I, Knutson H A, Charbonneau D (2007) Theoretical Spectral Models of the Planet HD 209458b with a Thermal Inversion and Water Emission Bands. *Astrophys. J. Lett.* 668:171-174.
40. Kratz D P (2008) The sensitivity of radiative transfer calculations to the changes in the HITRAN database from 1982 to 2004. *Journal of Quantitative Spectroscopy & Radiative Transfer* 109:1060-1080.
41. Burrows A, Sudarsky D, Lunine J I (2003) Beyond the T Dwarfs: Theoretical Spectra, Colors, and Detectability of the Coolest Brown Dwarfs. *Astrophys. J.* 596:587-596.
42. Fortney J J, Sudarsky D, Hubeny I, Cooper C S, Hubbard W B, Burrows A, Lunine J I (2003) On the Indirect Detection of Sodium in the Atmosphere of the Transiting Planet HD209458b. *Astrophys. J.* 589:615-622.
43. Howe A, Burrows A (2012) Theoretical Transit Spectra for GJ 1214b and Other 'Super-Earths'. *Astrophys. J.* 756:176-189.
44. Pont F, Knutson H A, Gilliland R L, Moutou C, Charbonneau D (2008) Detection of atmospheric haze on an extrasolar planet: the 0.55-1.05 μ m transmission spectrum of HD 189733b with the Hubble Space Telescope. *Mon. Not. R. Astron. Soc.* 385:109-118.
45. Grillmair C J, et al. (2008) Strong water absorption in the dayside emission spectrum of the planet HD189733b. *Nature* 456:767-769.
46. Lecavelier des Etangs A, Pont F, Vidal-Madjar A, Sing D (2008) Rayleigh scattering in the transit spectrum of HD 189733b. *Astron. Astrophys.* 481:83-86.
47. Snellen I A G, de Kok R J, de Mooij E J W, Albrecht S (2010) The orbital motion, absolute mass and high-altitude winds of exoplanet HD209458b. *Nature* 465:1049-1051.
48. Borucki W J, et al. (2010) Kepler Planet-Detection Mission: Introduction and First Results. *Science* 327:977-979.
49. Anderson D R, et al. (2013) Thermal emission at 3.6–8 μ m from WASP-19b: a hot Jupiter without a stratosphere orbiting an active star. *Mon. Not. R. Astron. Soc.* doi:10.1093/mnras/stt1140.
50. Deming D et al. (2013) Infrared Transmission Spectroscopy of the Exoplanets HD 209458b and XO-1b Using the Wide-Field Camera-3 on the Hubble Space Telescope. *Astrophys. J.* 774:95-112.
51. Werner, M W et al. (2004) The Spitzer Space Telescope Mission. *Astrophys. J. Suppl.* 154:1-9.
52. Burrows A, Sudarsky D, Hubeny I (2006) Theory for the Secondary Eclipse Fluxes, Spectra, Atmospheres, and Light Curves of Transiting Extrasolar Giant Planets. *Astrophys. J.* 650:1140-1149.
53. Burrows A, Budaj J, Hubeny I (2008) Theoretical Spectra and Light Curves of Close-in Extrasolar Giant Planets and Comparison with Data. *Astrophys. J.* 678:1436-1457.
54. Budaj J, Hubeny I, Burrows A (2012) Day and Night Side Cooling of a Strongly Irradiated Giant Planet. *Astron. Astrophys.* 537:A115 8 pp.
55. Spiegel D S, Burrows A (2010) Atmosphere and Spectral Models of the Kepler-field Planets HAT-P-7b and TrES-2. *Astrophys. J.* 722:871-879.
56. Hubeny I, Burrows A (2007) A Systematic Study of Departures from Chemical Equilibrium in the Atmospheres of Substellar Mass Objects. *Astrophys. J.* 669:1248-1261.
57. Knutson H A, Charbonneau D, Allen L E, Burrows A, Megeath S T (2008) The 3.6-8.0 μ m Broadband Emission Spectrum of HD 209458b: Evidence for an Atmospheric Temperature Inversion. *Astrophys. J.* 673:526-531.
58. Burrows A, Rauscher E, Spiegel D, Menou K (2010) Photometric and Spectral Signatures of 3D Models of Transiting Giant Exoplanets. *Astrophys. J.* 719:341-350.
59. Rowe J, et al. (2008) The Very Low Albedo of an Extrasolar Planet: MOST Space-based Photometry of HD 209458. *Astrophys. J.* 689:1345-1353.
60. Crossfield I J M, Barman T, Hansen B M S, Tanaka I, Kodama T (2012) Re-evaluating WASP-12b: Strong Emission at 2.315 μ m, Deeper Occultations, and an Isothermal Atmosphere. *Astrophys. J.* 760:140-155.
61. Madhusudhan N, Mousis O, Johnson T V, Lunine J I (2011) Carbon-rich Giant Planets: Atmospheric Chemistry, Thermal Inversions, Spectra, and Formation Conditions. *Astrophys. J.* 743:191-202.
62. Deming D et al. (2009) Discovery and Characterization of Transiting Super Earths Using an All-Sky Transit Survey and Follow-up by the James Webb Space Telescope. *PASP* 121:952-967.
63. Shabram M, Fortney J J, Greene T P, Freedman, R S (2011) Transmission Spectra of Transiting Planet Atmospheres: Model Validation and Simulations of the Hot Neptune GJ 436b for the James Webb Space Telescope. *Astrophys. J.* 727:65-74.
64. Angel J R P (2003) DARWIN/TPF and the Search for Extrasolar Terrestrial Planets. eds. in ESA Special Publications 539:221-230, eds. M. Fridlund, T Henning, H. Lacoste.
65. Tinetti G, et al. (2011) The science of EChO. The Astrophysics of Planetary Systems: Formation, Structure, and Dynamical Evolution, Proceedings of the International Astronomical Union, IAU Symposium 276:359-370.
66. Macintosh B et al. (2008) The Gemini Planet Imager: from science to design to construction. in Adaptive Optics Systems. Edited by Hubin, Norbert; Max, Claire E.; Wizinowich, Peter L. *Proc. SPIE* 7015:701518-701518-13.
67. Beuzit J-L et al. (2008) SPHERE: a planet finder instrument for the VLT. in Ground-based and Airborne Instrumentation for Astronomy II. Edited by McLean, Ian S.; Casali, Mark M. *Proc. SPIE* 7014:701418-701418-12.
68. Spergel D N, Gehrels N et al. (2013) Wide-Field InfraRed Survey Telescope – Astrophysics Focused Telescope Assets WFIRST-AFTA Final Report. <http://arxiv.org/abs/1305.5422> (astroph/1305.5422).

Figure Supplement to "Spectra as Windows into Exoplanet Atmospheres"

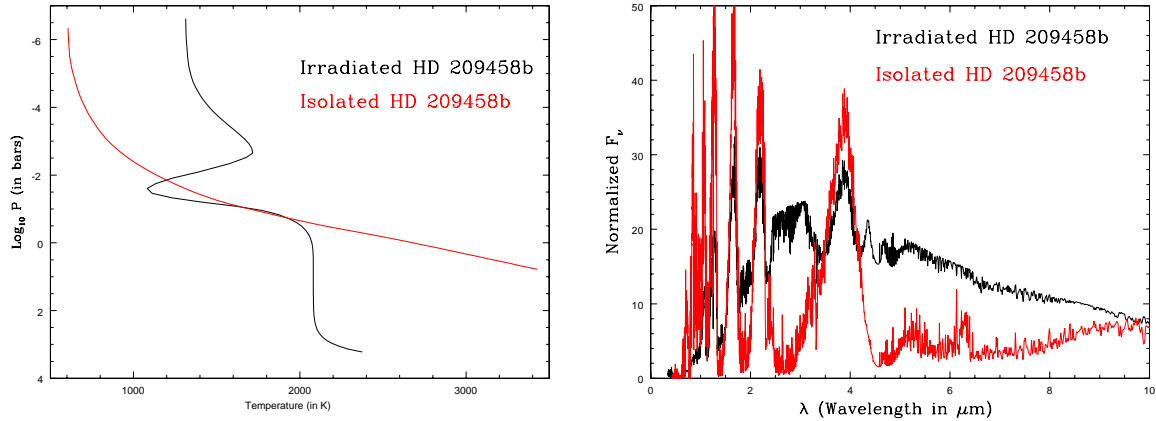


Fig. 4. Left: Shown are the temperature-pressure profiles for two models of HD 209458b. The black curve was generated including the stellar irradiation flux at the orbital distance of the planet and a token effective temperature (T_{eff}) of 200 K at the base. Note that T_{eff} for such a model reflects the *net* flux, not the emergent flux. The red curve is for an isolated model with roughly the same total emergent flux at an effective temperature T_{eff} of 1700 K. Despite having the same emergent flux, these temperature-pressure profiles are profoundly different. **Right:** The bottom panel depicts the corresponding normalized spectra, F_{ν} , versus wavelength (in microns). These spectra are vastly different, though the total emergent fluxes are the same, and demonstrate that one cannot assume that an equal emergent flux constraint will translate into useful spectra or colors. They also demonstrate that one must be careful when quoting an effective temperature, and not confute T_{eff} with an "equilibrium temperature," T_{eq} . See text for a discussion.

69. Knutson H A, Charbonneau D, Burrows A, O'Donovan F T, Mandushev G (2009) Detection of A Temperature Inversion in the Broadband Infrared Emission Spectrum of TrES-4. *Astrophys. J.* 691:866-874.
70. Fressin F, et al. (2010) The Broadband Infrared Emission Spectrum of the Exoplanet TrES-3. *Astrophys. J.* 711:374-379.
71. Croll B, Jayawardhana R, Fortney J J, Lafrenière D, Albert L (2010) Near-infrared Thermal Emission from TrES-3b: A Ks-band Detection and an H-band Upper Limit on the Depth of the Secondary Eclipse. *Astrophys. J.* 718:920-927.
72. Knutson H.A., et al. (2009) The 8 μ m Phase Variation of the Hot Saturn HD 149026b. *Astrophys. J.* 703:769-784.
73. Knutson H A, et al. (2012) 3.6 and 4.6 μ m Phase Curves and Evidence for Non-Equilibrium Chemistry in the Atmosphere of Extrasolar Planet HD 189733b. *Astrophys. J.* 754:22-37.
74. Agol E, et al. (2010) The Climate of HD 189733b from Fourteen Transits and Eclipses Measured by Spitzer. *Astrophys. J.* 721:1861-1877.
75. Charbonneau D, et al. (2008) The Broadband Infrared Emission Spectrum of the Exoplanet HD 189733b. *Astrophys. J.* 686:1341-1348.
76. Deming D, Harrington J, Seager S, Richardson L J (2006) Strong Infrared Emission from the Extrasolar Planet HD 189733b. *Astrophys. J.* 644:560-564.
77. Charbonneau D, et al. (2005) Detection of Thermal Emission from an Extrasolar Planet. *Astrophys. J.* 626:523-529.
78. Deming D, Seager S, Richardson L J, Harrington J (2005) Infrared radiation from an extrasolar planet. *Nature* 434:740-743.
79. O'Donovan F T, et al. (2010) Detection of Planetary Emission from the Exoplanet TrES-2 Using Spitzer/IRAC. *Astrophys. J.* 710:1551-1556.
80. Kipping D, Bakos G (2011) Analysis of Kepler's Short-cadence Photometry for TrES-2b. *Astrophys. J.* 733:36-52.
81. Croll B, Albert L, Lafrenière D, Jayawardhana R, Fortney J J (2010) Near-Infrared Thermal Emission from the Hot Jupiter TrES-2b: Ground-based Detection of the Secondary Eclipse. *Astrophys. J.* 717:1084-1091.
82. Christiansen J L, et al. (2010) Studying the Atmosphere of the Exoplanet HAT-P-7b Via Secondary Eclipse Measurements with EPOXI, Spitzer, and Kepler. *Astrophys. J.* 710:97-104.
83. Croll B, Lafrenière D, Albert L, Jayawardhana R, Fortney J J, Murray N (2011) Near-infrared Thermal Emission from WASP-12b: Detections of the Secondary Eclipse in Ks, H, and J. *Astron. J.* 131:30-41.
84. Cowan N B, et al. (2012) Thermal Phase Variations of WASP-12b: Defying Predictions. *Astrophys. J.* 747:82-98.
85. López-Morales M, et al. (2010) Day-side z'-band Emission and Eccentricity of WASP-12b. *Astrophys. J. Lett.* 716:36-40.
86. Nymeyer S, et al. (2011) Spitzer Secondary Eclipses of WASP-18b. *Astrophys. J.* 742:35-45.
87. Deming D, et al. (2011) Warm Spitzer Photometry of the Transiting Exoplanets CoRoT-1 and CoRoT-2 at Secondary Eclipse. *Astrophys. J.* 726:95-104.
88. Alonso R, et al. (2009) The secondary eclipse of CoRoT-1b. *Astron. Astrophys.* 506:353-358.
89. Gillon M, et al. (2009) VLT transit and occultation photometry for the bloated planet CoRoT-1b. *Astron. Astrophys.* 506:359-367.
90. Snellen I A G, de Mooij E J W, Albrecht S (2009) The changing phases of extrasolar planet CoRoT-1b. *Nature* 459:543-545.
91. Rogers J C, Apai D, López-Morales M, Sing D K, Burrows A (2009) Ks-Band Detection of Thermal Emission and Color Constraints to CoRoT-1b: A Low-Albedo Planet with Inefficient Atmospheric Energy Redistribution and a Temperature Inversion. *Astrophys. J.* 707:1707-1716.
92. Alonso R, et al. (2009) The secondary eclipse of the transiting exoplanet CoRoT-2b. *Astron. Astrophys.* 501:L23-L26.
93. Alonso R, et al. (2010) The secondary eclipse of the transiting exoplanet CoRoT-2b (Corrigendum). *Astron. Astrophys.* 512:1-1.
94. Snellen I A G, de Mooij E J W, Burrows A (2010) Bright optical day-side emission from extrasolar planet CoRoT-2b. *Astron. Astrophys.* 513:1-9
95. Gillon M, et al. (2010) The thermal emission of the young and massive planet CoRoT-2b at 4.5 and 8 μ m. *Astron. Astrophys.* 511:1-11
96. Lewis N K, et al. (2013) Orbital Phase Variations of the Eccentric Giant Planet HAT-P-2b. *Astrophys. J.* 766:95-117.
97. Machalek P, McCullough P R, Burke C J, Valenti J A, Burrows A, Hora J J (2008) Thermal Emission of Exoplanet XO-1b. *Astrophys. J.* 684:1427-1432.

98. Machalek P, McCullough P R, Burrows A, Burke C J, Hora J L, Johns-Krull C M (2009) Detection of Thermal Emission of XO-2b: Evidence for a Weak Temperature Inversion. *Astrophys. J.* 701:514-520.

99. Machalek, P et al. (2010) Thermal Emission and Tidal Heating of the Heavy and Eccentric Planet XO-3b. *Astrophys. J.* 711:111-118.

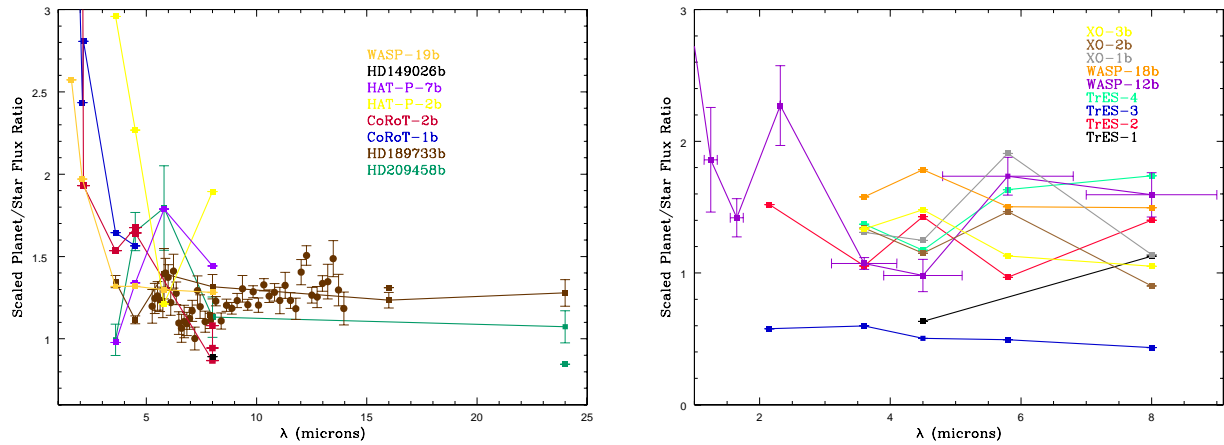


Fig. 5. Left: Planet/Star flux ratio data points at secondary eclipse for eight giant planets (WASP-19b, HD 149026b, HAT-P-7b, HAT-P-2b, CoRoT-2b, CoRoT-1b, HD 189733b, and HD 209458b), normalized to the corresponding ratio if both star and planet were black bodies at the corresponding measured stellar $T_{eff} = T_*$ and zero-albedo equilibrium temperature, $T_{eq} \left(= T_* \sqrt{\frac{R_*}{2a}} \right)$, respectively. The lines connect points for the same object. Most of the data are Spitzer/IRAC points, but points at shorter wavelengths, where available, are also included. For HD 209458b and HD 189733b, points at 16 and/or 24 microns are also given, along with points (unconnected and for comparison) derived from other reductions. To avoid further clutter, quoted error bars are given only for the IRS spectrometer data for HD 189733b and the Spitzer data for HD 209458b. **Right:** The same as on the top, but for XO-3b, XO-2b, XO-1b, WASP-18b, WASP-12b, TrES-4, TrES-3, TrES-2, and TrES-1. Error bars for only WASP-12b are given. The normalization provided helps to rationalize the interpretation potential of such photometric and low-resolution data and to facilitate planet-planet comparison. The data were taken from [69, 70, 71, 72, 73, 74, 75, 45, 76, 77, 57, 78, 79, 80, 81, 82, 83, 84, 60, 85, 86, 87, 88, 89, 90, 91, 92, 93, 94, 95, 96, 97, 98, 99, 49]. See text for a discussion.